

Discovery of 1,4-dihydroindeno[1,2-*c*]pyrazoles as a novel class of potent and selective checkpoint kinase 1 inhibitors

Yunsong Tong,* Akiyo Claiborne, Kent D. Stewart, Chang Park, Peter Kovar, Zehan Chen, Robert B. Credo, Wen-Zhen Gu, Stephen L. Gwaltney, II, Russell A. Judge, Haiying Zhang, Saul H. Rosenberg, Hing L. Sham, Thomas J. Sowin and Nan-horng Lin

Cancer Research, Global Pharmaceutical R&D, Abbott Laboratories, Abbott Park, IL 60064, USA

Received 19 December 2006; accepted 11 January 2007

Available online 17 January 2007

Abstract—A new class of checkpoint kinase 1 (CHK-1) inhibitors bearing a 1,4-dihydroindeno[1,2-*c*]pyrazole core was developed after initial hits from high throughput screening. The efficient hit-to-lead process was facilitated by X-ray crystallography and led to potent inhibitors (<10 nM) against CHK-1. X-ray co-crystal structures of bound inhibitors demonstrated that two sub-series of this class of compounds, exemplified by **21** and **41**, exhibit distinctive hydrogen bonding patterns in the specificity pocket of the active site. Two compounds, **41** and **43**, were capable of potentiating doxorubicin and camptothecin, both DNA-damaging agents, in cell proliferation assays (MTS and soft agar assays) and abrogating G2/M checkpoint in a mechanism-based FACS assay. © 2007 Elsevier Ltd. All rights reserved.

1. Introduction

A common choice to combat cancer is to use treatments with DNA-damaging potential. The effectiveness of these cytotoxic treatments, including ionized radiation (IR), UV radiation, and chemotherapy, however, has been hampered by severe side effects as well as drug resistance that patients may develop. Therefore, sensitizing the DNA-damaging treatments to make them more potent and/or more selective toward tumor cells could potentially offer a logical solution to this dilemma. Recently, there have been extensive studies on the role of checkpoint kinase 1 (CHK-1) in cell cycle in response to genotoxic stresses. These studies have demonstrated that inhibition of CHK-1 offers a mechanism for sensitizing various DNA-damaging therapies.¹

Human CHK-1 is a serine/threonine kinase with 476 amino acids.² Upon DNA damage, the upstream kinases ATR and/or ATM activate CHK-1 via phosphor-

ylation on its Ser345 and Ser317 sites.³ CHK-1 subsequently phosphorylates Cdc25A and induces its degradation, as a result, it inhibits the downstream cyclin E/Cdk2 or cyclin B/Cdk2 kinases, leading to cell cycle arrest at S phase or G2/M phase, respectively.⁴ Earlier studies have also suggested that CHK-1 phosphorylates Cdc25C on Ser216 and deactivates it, causing binding of Cdc25C to 14-3-3 proteins. This process inactivates cyclin B/Cdk2 and results in cells' arresting at G2/M checkpoint.⁵

Since tumor cells can arrest at different cell cycle checkpoints mediated by CHK-1 under genotoxic treatments, they have a chance to repair themselves. Thus, inhibition of CHK-1 to abrogate S and G2/M checkpoints will force tumor cells to undergo premature mitotic entry leading to cell death. A major difference between tumor cells and normal cells is that the former are often deficient of *p53*,⁶ which prevents them from arresting at G1 checkpoint. Whereas, in response to DNA damage, the normal cells are capable of arresting at G1 checkpoint through the *p53*-mediated pathway to ensure genomic integrity.⁷ This bias provides a potential therapeutic window for sensitizing DNA-damaging treatments of cancer using CHK-1 inhibitors. There have already been extensive reports on enhanced cell death in various cancer cell lines under genotoxic stresses by

Keywords: 1,4-Dihydroindeno[1,2-*c*]pyrazole; Checkpoint kinase 1 inhibitors; CHK-1; Potentiation or sensitization of DNA-damaging agents.

* Corresponding author. Tel.: +1 847 935 1252; fax: +1 847 935 5165; e-mail: yunsong.tong@abbott.com

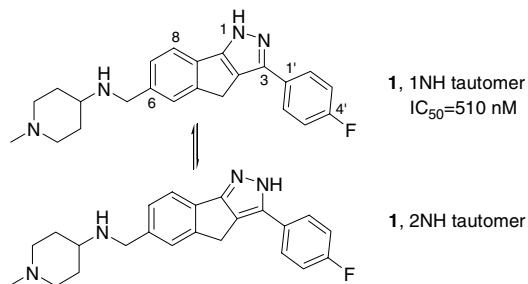


Chart 1.

eliminating CHK-1 via siRNA,⁸ anti-sense,⁹ and small molecule inhibitors.¹⁰ Here we report our discovery of 1,4-dihydroindeno[1,2-*c*]pyrazoles (referred to as tricyclic pyrazoles in this text) as a novel class of potent CHK-1 kinase inhibitors. The expedited hit-to-lead process was facilitated by X-ray crystallographic data, which will be discussed in detail. We will demonstrate that two sub-series of these inhibitors have unique interactions with the kinase specificity pocket in the ATP-binding site. Some molecules possess IC₅₀ values below 10 nM against CHK-1 and are capable of sensitizing doxorubicin and camptothecin, both DNA-damaging agents, in two cancer cell lines (HeLa and SW620) and abrogating G2/M checkpoint in H1299 cells.

A high throughput screen (HTS) resulted in hit molecules with a tricyclic pyrazole core as exemplified by **1** (Chart 1), with a CHK-1 IC₅₀ value of 510 nM. X-ray co-crystal structure of **1** in the CHK-1 active site indicates that the fluoro group resides in a region of limited volume where extra hydrogen bonding between the inhibitor and several polar residues of the backbone protein may be established. Further structural details will be addressed later in the text. Thus, our initial

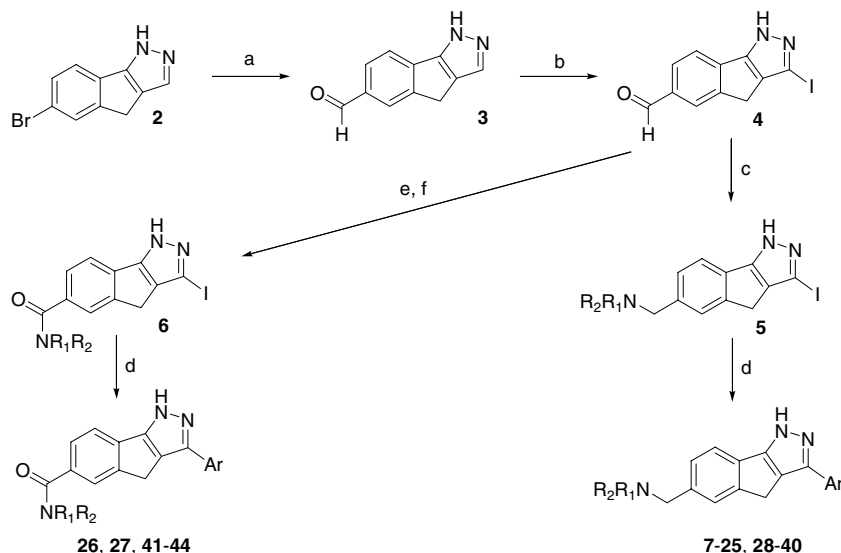
optimization of **1** was focused on modifying the fluoro group.

2. Chemistry

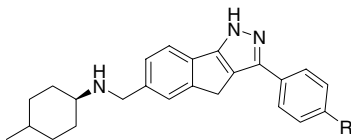
The synthesis is outlined in Scheme 1. A known molecule, 6-bromo-1,4-dihydro-indeno[1,2-*c*]pyrazole (**2**),¹¹ was lithiated and treated with DMF to afford aldehyde **3**. Subsequent iodination using NIS gave **4**. Reductive amination on the formyl group of **4** provided **5**, a key intermediate leading to final compounds **7–25** and **28–40** after coupling with aryl boronic acids or aryl pinacol borates under typical Suzuki reaction conditions assisted by microwave. Compound **4** also was oxidized followed by amide formation to give another key intermediate **6**. Final compounds **26**, **27**, and **41–44** were then prepared using similar Suzuki reactions.

3. Results and discussion

In order to simplify the synthetic work by using more commercially available reagents, the piperidylamino side chain at the 6 position of **1** was first replaced by 4-methylcyclohexylamino (**7** and **8** in Table 1). The result showed that such replacement maintained the enzymatic potency of **1**. In addition, the *cis/trans* stereochemistry of 4-methylcyclohexylamino had little effect on the potency. A series of functional groups were introduced at the 4' position to replace fluoro (**10–21** in Table 1). The replacements with a polar atom capped by an alkyl group (**15–17**) gave poor inhibitory activity. The unsubstituted amino moiety (**11**) also showed weak activity. However, the hydroxy group (**19**) boosted the potency of **1** by fourfold, although homologation (**13**) failed to deliver a better compound. The best replacement of the fluoro was a carboxylic acid:



Scheme 1. Synthesis of tricyclic pyrazoles. Reagents and conditions: (a) PhLi, *s*-BuLi, DMF, THF, -78°C to rt, 68%; (b) NIS, DMF, 80°C , 64%; (c) i—amine salts, K₂CO₃, EtOH, reflux; ii—NaBH₄; or i—amines, TsOH, toluene, reflux, ii—NaBH₄, EtOH, THF; (d) aryl boronic acids or aryl pinacol borates, 1 M Na₂CO₃, Pd(PPh₃)₂Cl₂, DME/EtOH/H₂O, microwave, 150°C ; (e) KH₂PO₄, H₂NSO₃H, NaClO₂, 1,4-dioxane, H₂O, 0°C , quan.; (f) 1° amines, EDC, HOBT, Et₃N, DMF, rt; or 2° amines, PyBOP, DIEA, DMF, rt.

Table 1. Optimizing the *para* substitution (R) of Ar


| Compound | Stereochemistry of cyclohexyl moiety | R | CHK-1 IC ₅₀ ^a (nM) |
|----------|--------------------------------------|----------------------|--|
| 7 | <i>cis</i> | F | 459 |
| 8 | <i>trans</i> | F | 814 |
| 9 | <i>trans</i> | H | 1473 |
| 10 | <i>trans</i> | Cl | 481 |
| 11 | <i>trans</i> | NH ₂ | 1042 |
| 12 | <i>trans</i> | CH ₂ COMe | 497 |
| 13 | <i>trans</i> | CH ₂ OH | 790 |
| 14 | <i>trans</i> | Me | 966 |
| 15 | <i>trans</i> | OEt | 1600 |
| 16 | <i>trans</i> | OCF ₃ | 2044 |
| 17 | <i>trans</i> | N(Me) ₂ | 5260 |
| 18 | <i>trans</i> | COOMe | 602 |
| 19 | <i>trans</i> | OH | 124 |
| 20 | <i>trans</i> | COOH | 22 |
| 21 | <i>cis</i> | COOH | 20 |

^a Compound concentration needed to cause 50% inhibition of Cdc25C phosphorylation in the presence of recombinant CHK-1 protein (ATP concentration is 5 μM).

compounds **20** and **21** exhibited approximately 20 nM inhibitory potency against CHK-1, a 25-fold improvement from the original HTS hit.

The much-improved potency of **21** can be rationalized with the help of the X-ray crystallographic structure of this molecule bound to the CHK-1 active site as shown in Figure 1a. The pyrazole, tautomer 2NH, makes two hydrogen bonding interactions with the hinge residues of CHK-1 by donating a H-bond to Glu85 O and accepting an H-bond from Cys87 NH, a feature we observed with compound **1**. A similar hinge binding pattern has been reported for other kinase inhibitors with the same or closely related tricyclic pyrazole core.¹² However, as compared to **1**, the carboxylic acid group of **21** accepts a key extra hydrogen bond (2.7 Å) from the positively charged amino group of Lys38, which forms a salt bridge to Glu55 (2.8 Å). Methylation of the acid of **21** to give the methyl ester **18** would eliminate this interaction and a 30-fold potency loss is observed. In addition, a bound water molecule, Wat 66, was observed to make a well-defined set of three hydrogen bonds between the carboxylic acid moiety and Glu55 and Asn59. The X-ray co-crystal structure further demonstrates that the amino side chain at the 6 position of these inhibitors points to the solvent-exposed area suggesting that this region of the inhibitor might prove amenable for modulation of biophysical characteristics of the series. The small impact of this side chain on binding affinity is supported by comparing **1** with **7** or **8**, **20** with **21**, and evident with compounds **22–27** in Table 2.

After identifying the carboxylic acid as an important fragment for binding in the polar region, we explored

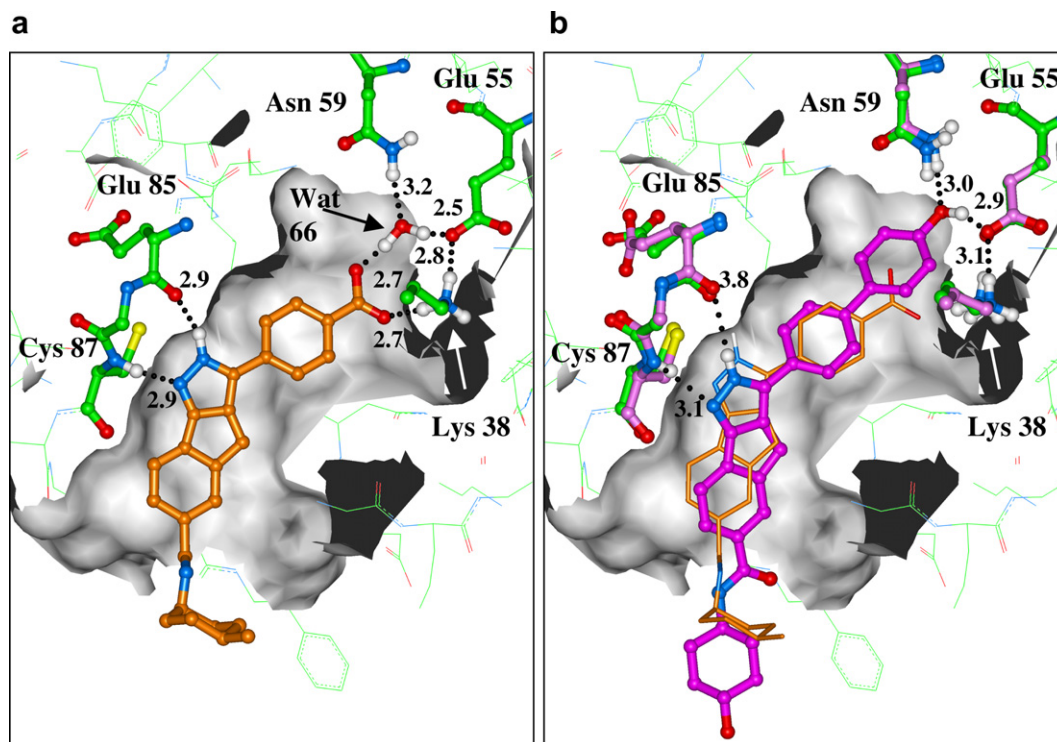
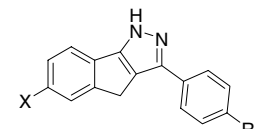


Figure 1. (a) (Ref. 13) X-ray structure of **21**, colored in orange, bound to CHK-1. Residues 38 (side chain only), 55, 59, 85, 86 (main chain only), and 87 of the protein are thick-bonded in green. The available volume in the active site is indicated with a gray surface. Protons were modeled using standard OH or NH distances. Numbers correspond to H-bond distances between heavy atoms. (b) (Ref. 13) X-ray structure of **41**, colored in pink, bound to CHK-1 overlaid on structure of Figure 1a by superposition of 264 pairs of alpha carbons with rms deviation of 0.4 Å. All atoms of highlighted residues showed shifts < 0.5 Å with the exception of Lys 38, whose side-chain amine shifted 0.7 Å between the two structures. The *trans*-aminocyclohexanol moiety of **41** is modeled as this was crystallographically disordered in the solvent accessible region.

Table 2. Further modifications of **20/21**


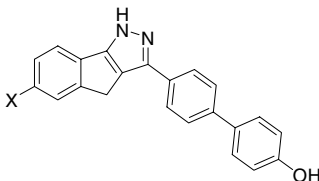
| Compound | X | R | CHK-1 IC ₅₀ (nM) |
|----------|---|--|--------------------------------|
| 22 | | COOH | 15 |
| 23 | | COOH | 7.9 |
| 24 | | COOH | 6.0 |
| 25 | | COOH | 15 |
| 26 | | COOH | 12 |
| 27 | | COOH | 12 |
| 28 | | CONH ₂ | 69 |
| 29 | | CONH ₂ | 29 |
| 30 | | SO ₂ NH ₂ | 535 |
| 31 | | SO ₂ NHCH ₂ CH ₂ OH | 8742 |
| 32 | | NHCOMe | 4825 |
| 33 | | CH ₂ NH ₂ | 1029 |
| 34 | | CONHSO ₂ Ph | 3064 |
| 35 | | CH ₂ CN | 1880 |
| 36 | | CH ₂ COOH | 6472 |

other functionalities mostly capable of accepting a hydrogen bond to replace the carboxylic acid, resulting in compounds **28–36** (Table 2). However, only the amide (**28** and **29**) appeared to be a reasonable, but not superior, substitute, while others led to much weaker inhibitors.

Another strategy was aimed at introducing a hydrogen bond between the inhibitor and Glu55 at the cost of

losing the carboxylic acid–Lys38 interaction **21** possesses. To accomplish that, an extra phenyl group was installed at the position of the carboxylic acid as a spacer to deliver a hydrogen bonding donor, a hydroxy group, toward Glu55. As a result, we discovered a new series of potent CHK-1 inhibitors shown in Table 3 featuring a bi-aryl phenol unit. These compounds (**37–44**) in general had higher binding affinity than the first generation inhibitors carrying the carboxylic acid. The most potent compound, **37**, had an IC₅₀ of 2.0 nM. Again, the left hand side chains at the 6 position showed little influence on enzyme inhibitory activity. X-ray co-crystal structure (Fig. 1b) of inhibitor **41** indicates that the hydroxy group replaces Wat 66 and forms its own hydrogen bonds to Glu55 (~2.9 Å) and Asn59 (~3.0 Å). Overlaying the crystal structures of **21** and **41** shown in Figure 1b revealed that the atomic position shifts in nearby protein residues were modest, typically <0.5 Å. The most dramatic structural changes observed for **41**, relative to **21**, were (1) an approximately 1 Å shift of the core tricyclic pyrazole unit to avoid clashing its extended right hand side with the polar residues, and (2) the above-mentioned Wat 66 replacement. The shift of the core unit is most evident in the hinge hydrogen bonding with the optimal distance of the H-bond donation to Glu85 O of 2.9 Å exhibited by **21** expanded to the much less optimal distance of 3.8 Å for **41**. The modest enhancement of potency of **41**, relative to **21**, suggests that whatever loss in binding energy caused by the decrease in hinge interaction may be compensated by some combination of additional hydrophobic binding by burial of the phenol aromatic unit and/or hydrogen bonding of the phenol hydroxy group. The hydroxyl group of the terminal phenol appeared to be optimal for interacting with CHK-1 since other polar replacements with H-bond donating capability and alkoxy groups led to either deteriorative or complete loss of potency (data not shown).

The compounds active in the enzymatic inhibition assay were further tested in two routine cellular assays. A cell proliferation assay (MTS assay) in HeLa cells (a human cervical cancer cell line) was used to measure the ability of CHK-1 inhibitors to sensitize a DNA-damaging agent, doxorubicin. An EC₅₀ was determined for the inhibitor as a single agent and the inhibitor in combination with doxorubicin (150 nM) with the ratio being a relative scale of an inhibitor's function to potentiate the DNA-damaging agent.¹⁴ In addition, a cell cycle analysis (FACS assay) in H1299 cells¹⁵ (a human lung cancer cell line) was carried out to determine if the mechanism of an inhibitor's ability to sensitize doxorubicin is through abrogation of G2/M checkpoint. In this assay, the EC₅₀ was either the concentration of a CHK-1 inhibitor that reduces doxorubicin (500 nM)-induced G2/M cell population by half, or it was measured in the absence of doxorubicin. As shown in Table 4, the CHK-1 inhibitors with carboxylic acid (**22–24**, **26**) or amide (**28**) moieties do not potentiate doxorubicin in the MTS assay. On the other hand, the inhibitors featuring the bi-aryl phenol unit (**37–44**) are active in the combination study in the MTS assay. Noticeably, some of those compounds (**37–40**) also show cyto-toxicity by

Table 3. A second series of potent inhibitors


| Compound | X | CHK-1 IC ₅₀ (nM) |
|----------|---|-----------------------------|
| 37 | | 2.0 |
| 38 | | 6.6 |
| 39 | | 3.9 |
| 40 | | 7.4 |
| 41 | | 6.2 |
| 42 | | 4.0 |
| 43 | | 13 |
| 44 | | 3.6 |

Table 4. Cellular activity of CHK-1 inhibitors

| Compound | MTS assay EC ₅₀ (μM) | | FACS assay EC ₅₀ (μM) | |
|----------|---------------------------------|-----------------------|----------------------------------|----------|
| | Single | With Dox ^a | Single | With Dox |
| 22 | >59 | >59 | NT ^b | NT |
| 23 | >59 | >59 | NT | NT |
| 24 | >59 | >59 | NT | NT |
| 26 | >59 | >59 | NT | NT |
| 28 | >59 | >59 | NT | NT |
| 37 | 4.7 | 0.81 | >10 | 1.1 |
| 39 | 2.3 | 2.0 | >10 | 0.83 |
| 40 | 4.0 | 2.9 | NT | NT |
| 41 | >59 | 1.8 | >10 | 0.77 |
| 43 | >59 | 1.1 | >10 | 0.98 |
| 44 | 25 | 14 | >10 | 2.7 |

^a Doxorubicin.^b Not tested.

themselves, an indication of possible off-target activities. Importantly, compounds **41** and **43** do demonstrate the desired cell proliferation profile, that is, non-toxic by themselves (EC₅₀ > 59 μM), but potent in combination with doxorubicin (EC₅₀ between 1 and 2 μM). The bi-aryl phenol compounds tested in the FACS assay also exhibit desirable behaviors, as they are able to abrogate G2/M checkpoint in combination with doxorubicin possessing EC₅₀ values below 1 μM (**41** and **43**). Meanwhile,

these compounds alone do not perturb normal cell cycle in the same assay (EC₅₀ > 10 μM).¹⁶ The overall lack of activity of the carboxylic acid bearing compounds (**22–24**, **26**) in the combination study of the cell proliferation assay may be attributed to their poor cellular permeability since Clog *P* values of these molecules are below 2. In contrast, the bi-aryl phenol inhibitors are active in this assay and have more favorable Clog *P* values of approximately 4.

To further demonstrate our CHK-1 inhibitors' ability to sensitize a DNA-damaging agent, we chose to measure the anti-proliferative EC₅₀ of camptothecin, a topoisomerase I inhibitor used in clinical practice, in the presence of a fixed concentration (3 and 10 μM) of compound **41** or **43** in a soft agar colony growth assay. The assay was run in SW620 cells (a human colon carcinoma cell line suitable for fast colony growth) with EC₅₀s determined for compound alone, camptothecin alone, and compound/camptothecin combo. The ratio of the EC₅₀ for camptothecin alone and the EC₅₀ for compound/camptothecin combo (referred to as the potentiation ratio) reflects the potentiation capability of the compounds. As shown in Table 5, both **41** and **43** display weak EC₅₀s (>25 μM) when tested alone, a sign of weak cyto-toxicity by themselves in line with the results from the corresponding MTS and FACS assays. Meanwhile, both compounds are able to sensitize the anti-proliferative activity of camptothecin with potentiation ratio being 4.9 for **41** and 2.0 for **43** when

Table 5. Potentiation of camptothecin (Cpt) by **41** and **43** in soft agar assay^a

| Compound alone | EC ₅₀ (μM) | | Potentiation ratio ^b |
|----------------|-----------------------|--|---------------------------------|
| | Cpt alone | Compd + Cpt | |
| 25.2 | 0.0021 | 0.00045 (3 μM 41) <0.00033 (10 μM 41) | 4.9 >6.7 |
| 28.2 | 0.0024 | 0.00012 (3 μM 43) 0.00033 (10 μM 43) | 2.0 6.5 |

^a See raw data displayed by error bars in Supplementary Information.^b Potentiation ratio, EC₅₀(Cpt alone)/EC₅₀(compd + Cpt).**Table 6.** Kinase selectivity profiles of **41** and **43**

| Ser/Thr kinases | IC ₅₀ (nM) ^a | |
|-----------------|------------------------------------|-----------------|
| | 41 | 43 |
| CHK-1 | 6.2 | 13 |
| CHK-2 | >50,000 | 10,300 |
| Aur1 | 8090 | NT ^b |
| CK2 | 41,000 | NT |
| PKA | >50,000 | >50,000 |
| PKCδ | >50,000 | >50,000 |
| PKCγ | >33,000 | 4900 |
| EMK | >50,000 | 4590 |
| ERK2 | >50,000 | >50,000 |
| SGK | 1320 | 15,000 |
| SRC | >50,000 | >50,000 |
| MARKAP2 | >50,000 | NT |
| AKT | 4430 | 1580 |
| CDC2 | >50,000 | >50,000 |

^a Radiometric assay (ATP concentration is 5 μM).^b Not tested.

compound concentration is 3 μ M. A dose-responsive enhancement of activity is also observed in the presence of 10 μ M of inhibitor. In this case, the potentiation ratio is increased to more than 6.7 for **41** and 6.5 for **43**.¹⁷

Compounds **41** and **43** were tested against a panel of thirteen other serine/threonine kinases to evaluate their selectivity profile (Table 6). Both molecules exhibit good selectivity as **41** and **43** are at least 213- and 122-fold more active against CHK-1 than any other kinase, respectively. This feature may be attributed to the hydrogen-bonding pattern these inhibitors display in the specificity pocket (i.e. the polar region) of the kinase active site.

4. Conclusions

In summary, starting from the HTS hit **1** with IC₅₀ value at 510 nM, we have discovered 1,4-dihydroindeno[1,2-*c*]pyrazoles as a new class of potent CHK-1 inhibitors (IC₅₀ = 2 nM for **37**). The hit-to-lead process was accomplished in an efficient fashion with the bound X-ray crystallographic data playing a key role. The compounds with carboxylic acid and bi-aryl phenol moieties show distinctive hydrogen bonding patterns in the polar region of the ATP binding site, yet they both demonstrate potent inhibition against CHK-1. The left hand side chains at the 6 position have a minimal impact on enzymatic potency and are designed to boost the solubility of the inhibitors. Most of the carboxylic acid bearing compounds have IC₅₀ values below 20 nM, meanwhile, the bi-aryl phenol compounds generally show IC₅₀ values below 10 nM. However, the former do not have potentiation activity in the MTS assay presumably due to their inadequate physical properties. The bi-aryl phenol inhibitors, represented by **41** and **43**, are selective against other serine/threonine kinases and exhibit profiles in both cell proliferation and cell cycle assays in the right direction, providing extra support to the notion that CHK-1 inhibitors may have potential therapeutic application in sensitizing DNA-damaging agents to combat cancer. Our findings warrant further optimization and investigation of this class of inhibitors.

5. Experimental

All commercially available chemical reagents were used without further purification unless otherwise noted. Flash chromatography was carried out using E. Merck silica gel 60 (230–400 mesh). Proton NMR data were recorded using a Varian Mercury 300 spectrometer or a Varian UNITY 400/500 spectrometer. Mass spectral data were collected using a Finnigan SSQ7000 GC/MS (ESI), or a Finnigan DCI/MS SSQ7000, or a JEOL SX102A HR/MS (FAB). Elemental analyses were performed by Robertson Microlit Laboratories or Quantitative Technologies, Inc. Preparative HPLC was performed on a Waters Novapak C18 column (100 \times 25 mm, 7 μ m particle size) using a gradient of 10–100% acetonitrile: 0.1% aqueous TFA over 10 min at a flow rate of 40 mL/min,

or a Phenomenex[®] Luna C18 (250 \times 21.2 mm) column with the same mobile phases (45 min run time). LC/MS was run on an Agilent 1100/Finnigan Navigator system with a YMC C18 column (50 \times 4.6 mm).

5.1. 1,4-Dihydro-indeno[1,2-*c*]pyrazole-6-carbaldehyde (**3**)

To a solution of 6-bromo-1,4-dihydro-indeno[1,2-*c*]pyrazole **2**¹¹ (0.100 g, 0.425 mmol) in THF (3 mL) at –78 °C was added 1.8 M PhLi in cyclohexane/ether (0.71 mL, 1.28 mmol) followed by 1.3 M *s*-BuLi in cyclohexane (0.98 mL, 1.28 mmol) 30 minutes later. The reaction mixture was stirred at –78 °C for 60 min and DMF (0.33 mL, 4.25 mmol) was added. The dry ice bath was removed after 30 min. After an additional 30 min, the reaction was quenched with water and extracted with EtOAc. The organic layer was washed with 50% brine, dried over MgSO₄, filtered, and concentrated. The concentrate was purified by flash chromatography eluted with EtOAc/hexane (7:3 to 8:2) to give 0.053 g (68%) of the desired product as brown solid. ¹H NMR (300 MHz, CD₃OD) δ 3.76 (s, 2H), 7.63 (s, 1H), 7.62–7.97 (m, 2H), 8.04 (s, 1H), 10.00 (s, 1H); MS (DCI/NH₃) *m/z*: 185.0 (M+H)⁺.

5.2. 3-Iodo-1,4-dihydro-indeno[1,2-*c*]pyrazole-6-carbaldehyde (**4**)

A suspension of **3** (7.90 g, 0.0429 mol) and *N*-iodosuccinimide (11.6 g, 0.0515 mol) in DMF (150 mL) was heated at 80 °C for 5.5 h. The reaction mixture was cooled and the solvent was evaporated. The concentrate was triturated with EtOAc and ether to give 7.20 g of brown solid as the desired product. The filtrate was concentrated and purified by flash chromatography eluted with EtOAc/hexane (7:3) to give 1.30 g of the desired product (combined yield: 64%). ¹H NMR (300 MHz, DMSO-*d*₆) δ 3.63 (s, 0.8H), 3.68 (s, 1.2H), 7.72 (d, *J* = 7.46 Hz, 0.5H), 7.83 (d, *J* = 7.80 Hz, 0.5H), 7.96 (m, 1 H), 8.07 (m, 1H), 10.03 (s, 1H), 13.45 (s, 0.6H), 13.72 (s, 0.4H); MS (DCI/NH₃) *m/z*: 310.9 (M+H)⁺.

5.3. General procedure for preparing intermediates **5**

Method A. To a suspension of **4** (0.0232 mol) in EtOH (500 mL) were added amine in the form of HCl salt (0.0579 mol) and potassium carbonate (0.0348 mol). The mixture was heated to refluxing overnight and cooled to room temperature. To the above yellow suspension was added NaBH₄ (0.0464 mol) in two portions and the reaction mixture was stirred overnight. The solid was filtered and washed with EtOH. The filtrate was concentrated and purified by flash chromatography to give the desired product. **Method B.** a mixture of **4** (3.22 mmol), free amine (9.66 mmol), and TsOH·H₂O (0.322 mmol) in toluene (50 mL) was heated to refluxing overnight. The solvent was evaporated. To the resulting residue were added EtOH (40 mL), THF (10 mL), and NaBH₄ (4.83 mmol) at room temperature. The mixture was stirred overnight and the resulting solid was filtered. The filtrate was concentrated, treated with 1 N HCl, and extracted with EtOAc. The aqueous layer was basified using 3 N NaOH and extracted with EtOAc. The organic

layer was dried over MgSO_4 , filtered, and concentrated. The residue was purified by flash chromatography to give the desired product.

5.4. General procedure for preparing intermediates 6

A mixture of **4** (3.00 g, 9.67 mmol), KH_2PO_4 (5.26 g, 0.0387 mol), and $\text{H}_2\text{NSO}_3\text{H}$ (1.41 g, 0.0145 mol) in 1,4-dioxane/ H_2O (100/30 mL) was stirred at 0 °C for 15 min. To this mixture was added NaClO_2 (1.14 g, 0.0126 mol) in H_2O (15 mL) dropwise. The reaction mixture was stirred for 15 min at 0 °C followed by the addition of NaHSO_3 (1.11 g, 0.0106 mol). The resulting suspension was warmed to room temperature and stirred for 1 h. The reaction mixture was treated with $\text{Na}_2\text{S}_2\text{O}_3$ solution and concentrated to remove most of the solvents. Water was added to the resulting slurry and the suspension was stirred for 1 h. The solid material was filtered, rinsed with water, and dried in a vacuum oven to give 3.49 g of the desired product as yellow solid. This product was used in the following step without further purification. ^1H NMR (300 MHz, $\text{DMSO}-d_6$) δ 3.57 (s, 2H), 7.67 (m, 1H), 7.98 (d, J = 7.80 Hz, 1H), 8.10 (s, 1H); MS (DCI/ NH_3) m/z : 327.0 ($\text{M}+\text{H}$) $^+$. The subsequent amide formation was carried out using two different methods. *Method A.* a mixture of the above carboxylic acid intermediate (0.150 mmol), HOBT (0.180 mmol), EDC (0.180 mmol), primary amine (0.180 mmol), and Et_3N (0.225 mmol) in DMF (3 mL) in a capped flask was stirred at room temperature for 24 h. The reaction mixture was diluted with EtOAc and washed with NaHCO_3 and brine. The organic layer was dried over MgSO_4 , filtered, concentrated, and triturated or purified by flash chromatography to give the desired product. *Method B.* a mixture of the above carboxylic acid intermediate (0.644 mmol), PyBOP (0.966 mmol), secondary amine (0.966 mmol), and diisopropylethylamine (2.25 mmol) in DMF (5 mL) was stirred at room temperature overnight. The reaction mixture was diluted with EtOAc and washed with water and NaHCO_3 . The organic layer was dried over MgSO_4 , filtered, concentrated, and purified by flash chromatography to give the desired product.

5.5. [3-(4-Fluoro-phenyl)-1,4-dihydro-indeno[1,2-*c*]pyrazol-6-ylmethyl]-(*cis*-4-methyl-cyclohexyl)-amine (**7**) TFA salt

A mixture of the corresponding intermediate **5** (30.0 mg, 0.0737 mmol), 4-fluorobenzene boronic acid (11.3 mg, 0.0811 mmol), Na_2CO_3 (1 M, 0.088 mL, 0.088 mmol), and $\text{Pd}(\text{PPh}_3)_2\text{Cl}_2$ (5.20 mg, 0.00737 mmol) in DME/ $\text{EtOH}/\text{H}_2\text{O}$ (7:2:3, 1.0 mL) in a capped 2 mL vial was heated to 150 °C for 300 s in a Smith Synthesizer (300 W). The reaction mixture was cooled using 40 psi pressurized air. Solvents were evaporated and the crude product was purified using preparative HPLC to give 3.0 mg of the desired product. ^1H NMR (300 MHz, CD_3OD) δ 1.03 (d, J = 6.78 Hz, 3H), 1.47–2.00 (m, 9H), 3.17–3.28 (m, 1H), 3.92 (s, 2H), 4.31 (s, 2H), 7.20–7.30 (m, 2H), 7.48–7.55 (m, 1H), 7.71 (s, 1H), 7.78–7.87 (m, 3H). HR/MS (FAB) calcd for $\text{C}_{24}\text{H}_{26}\text{FN}_3$ ($\text{M}+\text{H}$) $^+$ 376.2189; found 376.2177.

The remainders of the final products were synthesized via a Suzuki coupling reaction in the same manner. The microwave reactions were carried out with temperature and time in a range of 150–180 °C and 300–600 s, respectively. The reaction yields varied. To convert TFA salts of the final products into HCl salts, the TFA salts were dissolved in MeOH and treated with 1 M HCl/ether. Concentration of the suspension gave the desired product as an HCl salt.

5.6. 4-{6-[(*trans*-4-Methyl-cyclohexylamino)-methyl]-1,4-dihydro-indeno[1,2-*c*]pyrazol-3-yl}-benzoic acid (**20**) TFA salt

^1H NMR (300 MHz, CD_3OD) δ 0.95 (d, J = 6.44 Hz, 3H), 1.00–1.20 (m, 2H), 1.33–1.60 (m, 3H), 1.81–1.98 (m, 2H), 2.15–2.30 (m, 2H), 3.15 (m, 1H), 3.96 (s, 2H), 4.31 (s, 2H), 7.52 (m, 1H), 7.71 (m, 1H), 7.81 (d, J = 7.80 Hz, 1H), 7.90 (d, J = 8.81 Hz, 2H), 8.15 (d, J = 8.48 Hz, 2H). HR/MS (FAB) calcd for $\text{C}_{25}\text{H}_{27}\text{N}_3\text{O}_2$ ($\text{M}+\text{H}$) $^+$ 402.2182; found 402.2185.

5.7. 4-{6-[(*cis*-4-Methyl-cyclohexylamino)-methyl]-1,4-dihydro-indeno[1,2-*c*]pyrazol-3-yl}-benzoic acid (**21**) TFA salt

^1H NMR (300 MHz, CD_3OD) δ 1.04 (d, J = 7.12 Hz, 3H), 1.50–1.98 (m, 9H), 3.23 (m, 1H), 3.98 (s, 2H), 4.31 (s, 2H), 7.53 (d, J = 9.15 Hz, 1H), 7.73 (s, 1H), 7.82 (d, J = 7.80 Hz, 1H), 7.91 (d, J = 8.81 Hz, 2H), 8.15 (d, J = 8.48 Hz, 2H). MS (DCI/ NH_3) m/z : 402.2 ($\text{M}+\text{H}$) $^+$. Anal. ($\text{C}_{25}\text{H}_{27}\text{N}_3\text{O}_2 \cdot 1.35\text{TFA} \cdot 0.45\text{H}_2\text{O}$) C, H, N.

5.8. 4-{6-[(*trans*-4-Hydroxy-cyclohexylamino)-methyl]-1,4-dihydro-indeno[1,2-*c*]pyrazol-3-yl}-benzoic acid (**24**) HCl salt

^1H NMR (300 MHz, CD_3OD) δ 1.27–1.61 (m, 4H), 2.02–2.16 (m, 2H), 2.18–2.32 (m, 2H), 3.07–3.25 (m, 1H), 3.50–3.66 (m, 1H), 3.97 (s, 2H), 4.30 (s, 2H), 7.51 (dd, J = 7.80, 1.36 Hz, 1H), 7.71 (s, 1H), 7.81 (d, J = 7.80 Hz, 1H), 7.91 (d, J = 8.48 Hz, 2H), 8.15 (d, J = 8.48 Hz, 2H). HR/MS (FAB) calcd for $\text{C}_{24}\text{H}_{25}\text{N}_3\text{O}_3$ ($\text{M}+\text{H}$) $^+$ 404.1974; found 404.1987. Anal. ($\text{C}_{24}\text{H}_{25}\text{N}_3\text{O}_3 \cdot 2\text{HCl} \cdot 1.4\text{H}_2\text{O}$) C, H, N.

5.9. 4'-[6-(4-Hydroxy-cyclohexylmethyl)-1,4-dihydro-indeno[1,2-*c*]pyrazol-3-yl]-biphenyl-4-ol (**37**) TFA salt

^1H NMR (300 MHz, $\text{DMSO}-d_6$) δ 1.57 (m, 1H), 1.71–1.90 (m, 2H), 1.99 (m, 1H), 3.00 (m, 1H), 3.22 (s, br d, 2H), 3.34–3.45 (m, 2H), 3.96 (s, 2H), 4.38 (dd, J = 15.26, 4.75 Hz, 2H), 6.88 (d, J = 8.48 Hz, 2H), 7.48–7.59 (m, 3H), 7.70–7.78 (m, 4H), 7.87 (d, J = 8.48 Hz, 2H), 9.35 (s, br d, 1H), 9.61 (s, br d, 1H). MS (DCI/ NH_3) m/z : 438.2 ($\text{M}+\text{H}$) $^+$. Anal. ($\text{C}_{28}\text{H}_{27}\text{N}_3\text{O}_2 \cdot 2.85\text{TFA} \cdot 0.5\text{H}_2\text{O}$) C, H, N.

5.10. 4'-[6-[(*trans*-4-Hydroxy-cyclohexylamino)-methyl]-1,4-dihydro-indeno[1,2-*c*]pyrazol-3-yl]-biphenyl-4-ol (**39**) TFA salt

^1H NMR (300 MHz, CD_3OD) δ 1.24–1.63 (m, 4H), 1.99–2.16 (m, 2H), 2.17–2.34 (m, 2H), 3.06–3.25 (m,

1H), 3.49–3.67 (m, 1H), 3.93 (s, 2H), 4.28 (s, 2H), 6.89 (d, $J = 8.81$ Hz, 2H), 7.43–7.58 (m, 3H), 7.63–7.76 (m, 3H), 7.76–7.93 (m, 3H). MS (DCI/NH₃) m/z : 452.2 (M+H)⁺. Anal. (C₂₉H₂₉N₃O₂·2TFA·1.5H₂O) C, H, N.

5.11. 3-(4'-Hydroxy-biphenyl-4-yl)-1,4-dihydro-indeno[1,2-c]pyrazole-6-carboxylic acid (*trans*-4-hydroxy-cyclohexyl)-amide (41) TFA salt

¹H NMR (500 MHz, DMSO-*d*₆) δ 1.18–1.33 (m, 2H), 1.34–1.49 (m, 2H), 1.85 (t, $J = 13.26$ Hz, 4H), 3.36–3.46 (m, 1H), 3.68–3.81 (m, 1H), 3.96 (s, 2H), 4.53 (s, 1H), 6.88 (d, $J = 8.42$ Hz, 2H), 7.57 (d, $J = 8.11$ Hz, 2H), 7.74 (d, $J = 6.86$ Hz, 2H), 7.80–7.96 (m, 3H), 8.04 (s, 1H), 8.20 (d, $J = 7.80$ Hz, 1H), 9.58 (s, 1H), 13.36 (s, 1H). MS (DCI/NH₃) m/z : 466.2 (M+H)⁺. Anal. (C₂₉H₂₇N₃O₃·0.75TFA·0.35H₂O) C, H, N.

5.12. 3-(4'-Hydroxy-biphenyl-4-yl)-1,4-dihydro-indeno[1,2-c]pyrazole-6-carboxylic acid (pyridin-4-ylmethyl)-amide (43) TFA salt

¹H NMR (500 MHz, DMSO-*D*₆) δ 3.99 (s, 2H), 4.70 (d, $J = 5.61$ Hz, 2H), 6.88 (d, $J = 8.42$ Hz, 2H), 7.58 (d, $J = 8.73$ Hz, 2H), 7.74 (d, $J = 8.11$ Hz, 2H), 7.79 (d, $J = 6.86$ Hz, 3H), 7.88 (d, $J = 8.11$ Hz, 2H), 7.98 (d, $J = 7.80$ Hz, 1H), 8.14 (s, 1H), 8.76 (d, $J = 5.61$ Hz, 2H), 9.32 (t, $J = 5.77$ Hz, 1H), 9.59 (s, br d, 1H). MS (DCI/NH₃) m/z : 459.2 (M+H)⁺. Anal. (C₂₉H₂₂N₄O₂·1.75TFA·0.7H₂O) C, H, N, F.

5.13. [3-(4'-Hydroxy-biphenyl-4-yl)-1,4-dihydro-indeno[1,2-c]pyrazol-6-yl]-(4-hydroxy-piperidin-1-yl)-methanone (44) TFA salt

¹H NMR (300 MHz, CD₃OD) δ 1.44–1.66 (m, 2H), 1.81–2.01 (m, 2H), 3.32–3.42 (m, 2H), 3.75 (m, 1H), 3.90 (m, 1H), 3.96 (s, 2H), 4.22 (m, 1H), 6.88 (d, $J = 8.81$ Hz, 2H), 7.45 (d, $J = 7.80$ Hz, 1H), 7.53 (d, $J = 8.81$ Hz, 2H), 7.65 (s, 1H), 7.70 (d, $J = 8.48$ Hz, 2H), 7.78–7.85 (m, 3H). MS (DCI/NH₃) m/z : 452.1 (M+H)⁺. Anal. (C₂₈H₂₅N₃O₃·1.9TFA·0.3H₂O) C, H, N.

5.14. CHK-1 enzymatic inhibition assay

The Chk1 enzymatic assay was carried out using a recombinant CHK-1 kinase domain protein with amino acids from residue 1–289. A human biotinylated Cdc25c peptide was used as substrate (Synpep Catalog# 02-1-22-1-ABB). The reaction mixture contained 25 mM Hepes at pH 7.4, 10 mM MgCl₂, 0.08 mM Triton X-100, 0.5 mM DTT, 5 μ M ATP, 4 nM ³³P ATP, 5 μ M Cdc25c peptide substrate, and 5 nM of the recombinant Chk1 protein. For potent compound with K_i below 1 nM, 0.5 nM of the recombinant CHK-1 protein and 8 nM of ³³P were used. The concentration of the vehicle, DMSO, in the final reaction is 2%. After 30 min at room temperature, the reaction was stopped by addition of equal volume of 4 M NaCl and 0.1 M EDTA (pH 8.0). A 40 μ L aliquot of the reaction was added to a well in a Flash Plate (NEN Life Science

Products, Boston, MA) containing 160 μ L of phosphate-buffered saline (PBS) without calcium chloride, and magnesium chloride and incubated at room temperature for 10 min. The plate was then washed 3 times in PBS with 0.05% Tween 20 and counted in a Packard TopCount counter (Packard BioScience Company, Meriden, CT).

5.15. Kinase (Ser/Thr) selectivity assays

The assays were run using a radioactive-based assay platform. CHK-1 inhibitors were incubated with biotinylated substrate peptide (2 μ M), γ -[³³P]ATP (5 μ M), and a kinase assay buffer for 30 min and the reaction was stopped by 100 mM EDTA. The mixture was transferred to streptavidin-coated 384-well FlashPlates (Perkin-Elmer). The plates were washed and the peptide phosphorylation count was read using a TopCount microplate reader.

5.16. Cell proliferation assay (MTS assay)

Hela cells were inoculated into a 96-well microtiter plate and cultured overnight at 37 degrees. The CHK-1 inhibitor was pre-mixed with culture medium before being added to the cells and the cells were continued to incubate for 48 h. For the doxorubicin combination study, the cell culture medium also contained a fixed concentration of 150 nM Doxorubicin. After the treatment, MTS reagents that measure the amount of live cells (Promega, Madison, WI) were added to the cells and allowed to develop for 20 min to 2 h. Colorimetric measurement was taken at 490 nm on Spectra MAX 190 from Molecular Devices (Sunnyvale, CA). For combination study, the base line of the regression was adjusted to the inhibition level determined for 150 nM doxorubicin alone.

5.17. Cell cycle analysis (FACS)

Cells were treated with CHK-1 inhibitors and trypsinized, and added to the tubes with the medium and PBS. The cells were washed in PBS and fixed in 70% ethanol. The fixed cells were washed again twice with PBS and treated with RNase A at 37 °C for 30 min. The cells were stained with propidium iodide and incubated in the dark for 60 min or overnight before analysis. The samples were analyzed through flow cytometry using fluorescence-activated cell sorting (FACS) manufactured by BD Bioscience (San Jose, CA) using the Cell-Quest program.

5.18. Cell proliferation assay (soft agar assay)

In 12-well plates, the bottom layer contained 0.5 mL of 0.7% agar with either increasing dose of camptothecin or camptothecin in combination with a CHK-1 inhibitor, the top layer contained 0.5 mL of 0.35% agar with the medium mixed with 5000 cells/well of SW620 cells. Colonies were incubated for 14 days, stained with iodine-tetrazolium at 0.5 μ g/mL overnight, and counted using a Sony CCD camera linked to the Image-Pro Plus software.

Acknowledgments

The authors thank Drs. Nobuhiko Iwasaki, Paul Rafferty, Keith Wood, Gary Wang, and Zhan Xiao for helpful discussions.

Supplementary data

See raw data for FACS and soft agar assays, and spectral data for compounds **8–19**, **22**, **23**, **25–36**, **38**, **40**, **42** in Supplementary Information. Supplementary data associated with this article can be found, in the online version, at [doi:10.1016/j.bmc.2007.01.012](https://doi.org/10.1016/j.bmc.2007.01.012).

References and notes

- Reviews: (a) Zhou, B. B.; Bartek, J. *Nat. Rev. Cancer* **2004**, *4*, 1–10; (b) Luo, Y.; Levenson, J. D. *Expert Rev. Anticancer Ther.* **2005**, *5*, 333–342; (c) Tao, Z.-F.; Lin, N.-H. *Anticancer Agents Med. Chem.* **2006**, *6*, 377–388.
- Sanchez, Y.; Wong, C.; Thomas, R. S.; Richman, R.; Wu, Z.; Piwnica-Worms, H.; Elledge, S. J. *Science* **1997**, *277*, 1497–1501.
- Reviews: (a) Abraham, R. T. *Genes Dev.* **2001**, *15*, 2177–2196; (b) Shiloh, Y. *Nat. Rev. Cancer* **2003**, *3*, 155–168.
- (a) Xiao, Z.; Chen, Z.; Gunasekera, A. H.; Sowin, T. J.; Rosenberg, S. H.; Fesik, S.; Zhang, H. *J. Biol. Chem.* **2003**, *278*, 21767–21773; (b) Mailand, N.; Falck, J.; Lukas, C.; Syljuåsen, R. G.; Welcker, M.; Bartek, J.; Lukas, J. *Science* **2000**, *288*, 1425–1429; (c) Uto, K.; Inoue, D.; Shimuta, K.; Nakajo, N.; Sagata, N. *EMBO J.* **2004**, *23*, 3386–3396; (d) Zhao, H.; Watkins, J. L.; Piwnica-Worms, H. *Proc. Natl. Acad. Sci. U.S.A.* **2002**, *99*, 14795–14800.
- Peng, C.-Y.; Graves, P. R.; Thomas, R. S.; Wu, Z.; Shaw, A. S.; Piwnica-Worms, H. *Science* **1997**, *277*, 1501–1505.
- Greenblatt, M. S.; Bennett, W. P.; Hollstein, M.; Harris, C. C. *Cancer Res.* **1994**, *54*, 4855–4878.
- (a) Powell, S. N.; DeFrank, J. S.; Connell, P.; Eogan, M.; Pfeffer, F.; Dombkowski, D.; Tang, W.; Friend, S. *Cancer Res.* **1995**, *55*, 1643–1648; (b) Kuerbitz, S. J.; Plunkett, B. S.; Walsh, W. V.; Kastan, M. B. *Proc. Natl. Acad. Sci. U.S.A.* **1992**, *89*, 7491–7495.
- (a) Chen, Z.; Xiao, Z.; Chen, J.; Ng, S.-C.; Sowin, T.; Sham, H.; Rosenberg, S.; Fesik, S.; Zhang, H. *Mol. Cancer Ther.* **2003**, *2*, 543–548; (b) Flatten, K.; Dai, N. T.; Vroman, B. T.; Loegering, D.; Erlichman, C.; Karnitz, L. M.; Kaufmann, S. H. *J. Biol. Chem.* **2005**, *280*, 14349–14355.
- Wang, H.; Wang, X.; Zhou, X.-Y.; Chen, D. J.; Li, G. C.; Iliakis, G.; Wang, Y. *Cancer Res.* **2002**, *62*, 2483–2487.
- (a) Huang, S.; Garbaccio, R. M.; Fraley, M. E.; Steen, J.; Kreatsoulas, C.; Hartman, G.; Stirdivant, S.; Drakas, B.; Rickert, K.; Walsh, E.; Hamilton, K.; Buser, C. A.; Hardwick, J.; Mao, X.; Abrams, M.; Beck, S.; Tao, W.; Lobell, R.; Sepp-Lorenzino, L.; Yan, Y.; Ikuta, M.; Murphy, J. Z.; Sardana, V.; Munshi, S.; Kuo, L.; Reilly, M.; Mahan, E. *Bioorg. Med. Chem. Lett.* **2006**, *16*, 5907–5912; (b) Lin, N.-H.; Xia, P.; Kovar, P.; Park, C.; Chen, Z.; Zhang, H.; Rosenberg, S. H.; Sham, H. L. *Bioorg. Med. Chem. Lett.* **2006**, *16*, 421–426; (c) Li, G.; Hasvold, L. A.; Tao, Z.-F.; Wang, G. T.; Gwaltney, S. L.; Patel, J.; Kovar, P.; Credo, R. B.; Chen, Z.; Zhang, H.; Park, C.; Sham, H. L.; Sowin, T.; Rosenberg, S. H.; Lin, N.-H. *Bioorg. Med. Chem. Lett.* **2006**, *16*, 2293–2298; (d) Ni, Z.-J.; Barsanti, P.; Brammeier, N.; Diebes, A.; Poon, D. J.; Ng, S.; Pecchi, S.; Pfister, K.; Renhowe, P. A.; Ramurthy, S.; Wagman, A. S.; Bussiere, D. E.; Le, V.; Zhou, Y.; Jansen, J. M.; Ma, S.; Gesner, T. G. *Bioorg. Med. Chem. Lett.* **2006**, *16*, 3121–3124; (e) Wang, G. T.; Li, G.; Mantel, R. A.; Chen, Z.; Kovar, P.; Gu, W.; Xiao, Z.; Zhang, H.; Sham, H. L.; Sowin, T.; Rosenberg, S. H.; Lin, N.-H. *J. Med. Chem.* **2005**, *48*, 3118–3121; (f) Foloppe, N.; Fisher, L. M.; Howes, R.; Kierstan, P.; Potter, A.; Robertson, A. G. S.; Surgenor, A. E. *J. Med. Chem.* **2005**, *48*, 4332–4345; (g) Jiang, X.; Zhao, B.; Britton, R.; Lim, L. Y.; Leong, D.; Sanghera, J. S.; Zhou, B.-B. S.; Piers, E.; Andersen, R. J.; Roberge, M. *Mol. Cancer Ther.* **2004**, *3*, 1221–1227.
- Doyle, K.; Rafferty, P.; Steele, R.; Turner, A.; Wilkins, D.; Arnold, L. Therapeutic agents. US 6297238.
- (a) Nugiel, D. A.; Vidwans, A.; Etzkorn, A.-M.; Rossi, K. A.; Benfield, P. A.; Burton, C. R.; Cox, S.; Doleniak, D.; Seitz, S. J. *J. Med. Chem.* **2002**, *45*, 5224–5232; (b) Dinges, J.; Akritopoulou-Zanze, I.; Arnold, L. D.; Barlozzari, T.; Bousquet, P. F.; Cunha, G. A.; Ericsson, A. M.; Iwasaki, N.; Michaelides, M. R.; Ogawa, N.; Phelan, K. M.; Rafferty, P.; Sowin, T. J.; Stewart, K. D.; Tokuyama, R.; Xia, Z.; Zhang, H. Q. *Bioorg. Med. Chem. Lett.* **2006**, *16*, 4371–4375.
- See coordinates in PDB. Codes: 2E9O for **21**; 2E9N for **41**.
- For combination study, the base line of the regression was adjusted to the inhibition level determined for 150 nM doxorubicin alone, a concentration known to cause G2/M arrest in HeLa cells.
- H1299 cell line provided faster cell growth and better cell cycle profiles.
- See representative raw data curves for **43** in Supplementary Information.
- See raw data displayed by error bars in Supplementary Information.